J.W. Hightower, W.N. Delgass, E. Iglesia and A.T. Bell (Eds.)
11th International Congress on Catalysis - 40th Anniversary
Studies in Surface Science and Catalysis, Vol. 101

The Development of Strong Acidity by Non-Framework Aluminum in H-USY Determined by Al XAFS Spectroscopy

D.C. Koningsberger[a] and J.T. Miller[b]

[a]Department of Inorganic Chemistry and Catalysis; Utrecht University; PO Box 80083; 3508 TB Utrecht THE NETHERLANDS

[b]AMOCO; PO Box 3011, Mail Station H-9; Naperville, Il 60566-7011 USA

The local structure of framework and non-framework Al in dealuminated, ultrastable H-Y (H-USY) zeolite has been determined by low energy Al XAFS spectroscopy. By determining the fraction of lattice Al from ^{27}Al NMR and XRD, the Al-O distances of both structural (tetrahedral) and non-structural (octahedral) Al can be determined. Compared to an Al-O distance of 1.69 Å in H-Y, steam dealumination results in a slight decrease in the tetrahedral Al-O distance to 1.67 Å. In addition, the octahedral Al-O distance in H-Y is 1.91 Å and decreases to 1.84 Å in H-USY. A large increase in the intensity of the whiteline in H-USY indicates that the lattice Al has a higher positive charge than in H-Y. The XAFS results suggest that steam dealumination results in the formation of octahedral, non-framework Al at ion exchanged sites which withdraw electron density from the tetrahedral Al through the lattice oxygen ions. The results of this study, support the model that non-framework Al cations withdraw electron density from the lattice oxygen increasing the strength of the acid sites.

1. INTRODUCTION

Solid acid catalysts play a prominent role in the development of catalytic processes in the petrochemical industries. Current industrial processes are dominated by zeolite catalysts. The structure of zeolites is composed of oxide tetrahedra of silicon and aluminum. Charge balance requires that for each aluminum there is one cation. For most hydrocarbon reactions, alkali metal zeolites, for example Na-Y, are relatively unreactive. Exchange of the alkali ions by ammonium ions with subsequent calcination to produce H-Y increases the catalytic activity compared to Na-Y. It is generally accepted that in acidic zeolites, the active site is a Bronsted acid localized on an oxygen ion coordinated to aluminum.

Controlled hydrothermal decomposition of NH_4-Y results in increased hydrothermal stability, i.e., ultrastable Y, or H-USY, and partial dealumination with the formation of non-framework Al [1]. Despite fewer acid sites, H-USY displays greatly enhanced catalytic activity compared to H-Y [2]. Several factors may contribute to the increased acidity. For example, isolated Al, e.g., those with no second nearest neighbor Al, are more strongly acidic [3,4]. In addition, non-framework Al may withdraw electron density from the lattice oxygen increasing the acid strength [5,6]. The non-framework Al ions may be located in the sodalite cages [5], or may be Lewis acid sites near the (structural) Bronsted site [6,7]. Alternatively, non-framework aluminum may form amorphus silica-alumina within the zeolite pores which

is more catalytically active than the zeolite acid sites [8]. Nonstructural Al has also been proposed to produce Lewis acid sites which may promote hydride abstraction and initiate catalytic reactions [9].

While much is known about the changes in the catalytic and spectroscopic properties which occur upon dealumination, little is known about local structural changes at the active site, for example, changes in the Al-O bond distance, or changes in the electron density of the aluminum ion. Recent XAFS studies on the structural and electronic properties of Al ions in the Y zeolite have shown that the Al-O bond distance is insensitive to the acidity of the zeolite [10,11]. However, the Al whiteline intensity is strongly influenced by the acidity. The whiteline intensity of ion exchanged NaY increases as the charge on the cation increases from H-Y < H-CaY < H-LaY and parallels the catalysts acidity [11]. A higher white line intensity indicates a higher positive charge on the lattice Al ion. The influence of the cation on the charge of the Al ion suggests that polyvalent cations withdraw electron density from the Al through the lattice oxygens. The correlation of the whiteline intensity with the acidity indicates that the origin of the enhanced acid strength is due to the withdrawal of the electron density from the acidic hydroxyl groups by the nearby polycation.

In the present study, the effect of steam dealumination on the tetrahedral and octahedral Al-O bond distances in H-USY has been determined by Al XAFS spectroscopy. By combination of X-ray diffraction and ^{27}Al NMR to determine the fraction of Al in the lattice, it is possible to determine the Al-O bond distances of both the structural and non-structural Al. In the near edge spectra the presence of both tetrahedral and octahedral coordinated Al can be resolved. Moreover, the whiteline intensity of the tetrahedral Al in H-USY is much larger than that in H-Y.

2. EXPERIMENTAL

Na-Y was a commercial zeolite (LZ-Y54) obtained from UOP. The sample crystallinity was confirmed by XRD and had a unit cell dimension of 24.676 Å. NH_4-Y was prepared by ammonium exchange of Na-Y (150 g of Na-Y was exchanged 10 times with 1 L of 2 M NH_4NO_3 at 80°C). H-Y was prepared by careful calcination of NH_4-Y (heating at 1 °C/min to 300°C in dry, flowing air followed by 4 h at 300°C). The loss of ammonia was confirmed by NH_3 TPD. The crystallinity by XRD was 98% based on Na-Y as a standard, and the unit cell dimension was 24.643 Å. The contraction in the unit cell dimension also confirms the loss of ammonia. The elemental analysis was 11.5 wt% Al and 0.13 wt% Na and the N_2 micropore volume was 0.348 cc/g. H-USY (LZ-Y84) was also a commercial zeolite and was calcined at 450°C for 4 h. The crystallinity by XRD was 90% and the unit cell dimension was 24.525 Å. The elemental analysis was 10.6% Al and 0.10% Na, and the N_2 micropore volume of 0.266 cc/g. Hydrated zeolites were analyzed by XRD and Al NMR using standard methods.

EXAFS measurements were performed at the soft X-ray XAFS station 3.4 of the SRS at Daresbury (UK). This station is equipped with a quartz, double crystal monochromator, and harmonic contamination of the X-ray beam was minimized by collimating mirrors. The estimated resolution was 1.5 eV at the Al K-edge (1559 eV). Data were simultaneously collected with a fluorescence and electron yield detector. Six scans were averaged in order to minimize both high and low frequency noise. The electron yield spectra indicate no distortion of the absorption coefficient in the near edge region while the fluorescence spectra were reduced in amplitude due to absorption by the sample. The instrumental background

in the EXAFS region of electron yield spectra was unreliable, however, requiring the EXAFS data to be collected in fluorescence. Sample preparation, reference compounds, experimental conditions and standard procedures for analysis of XAFS data have previously been reported [10]. The data were analyzed using the latest version of the Utrecht University XAFS Data Analysis Program (XDAP) which allows for fitting in r-space both on the imaginary and the absolute part of the of the Fourier transform.

3. RESULTS

3.1 XRD

From the unit cell size, a_o, the number of Al/unit cell, i.e., the amount of structural, tetrahedral Al, is calculated [12]:

$$\text{Al/unit cell} = (a_o - 24.191)/0.00868$$

In NaY there are 56 Al/unit cell, in H-Y there are 52 Al/unit cell, and in H-USY there are 38 Al/unit cell. In order to determine the fraction of framework Al in the sample, the Al/unit cell is corrected by the sample crystallinity. For example, in Na-Y (100% crystalline) there are 56 Al/unit cell. For H-USY, which is prepared from hydrothermal dealumination of ammonium exchanged NaY, there are 38 Al/unit cell, but the crystallinity is 90%. The amount of structural, tetrahedral Al is equal to about 60% (38/56 x 0.9), or 40% of the Al in H-USY is non-structural.

3.2 NMR

The ^{27}Al NMR spectra of H-Y and H-USY are shown in Figure 1. For H-Y, Figure 1a, 85% of the Al is in tetrahedral coordination (60 ppm) and 15% of the Al is in octahedral coordination (0 ppm) (13-15). For H-USY, Figure 1b, the fraction of Al in tetrahedral coordination is much lower, about 40%. The fraction of Al in octahedral coordination has increased to 45% and the remaining intensity at about 30 ppm accounts for 15% of the Al intensity. The 30 ppm resonance has previously been assigned to non-structural penta-coordinate Al (13), or non-framework Al in a distorted tetrahedral coordination (14).

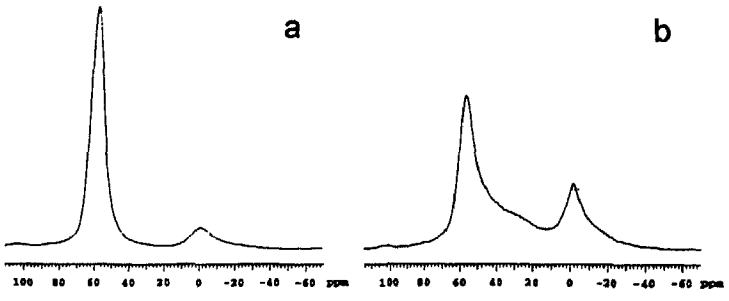

Figure 1. ^{27}Al NMR Spectra of a.) H-Y and b.) H-USY

3.3 X-ray Absorbtion Near Edge Spectra

The whiteline can be assigned to a 1s to 3p transition, e.g., for tetrahedral Al the transition is $1a_g$ to t_2 and for octahedral Al, $1a_g$ to t_{1u}. The normalized near edge spectra for H-Y (dotted line) and H-USY (solid line) are given in Figure 2. The position of the whiteline beyond the edge absorption edge is ca. 2 eV for Al_{tet} and 6 eV Al_{oct}. The edge positions are sufficiently different that a clear distinction can be made. In H-Y the near edge is more typical for the Al_{tet}, while both Al_{tet} and Al_{oct} are present in H-USY. Although there is only about 60% Al_{tet} in H-USY, the white line intensity is much higher than that in H-Y with about 90% Al_{tet}.

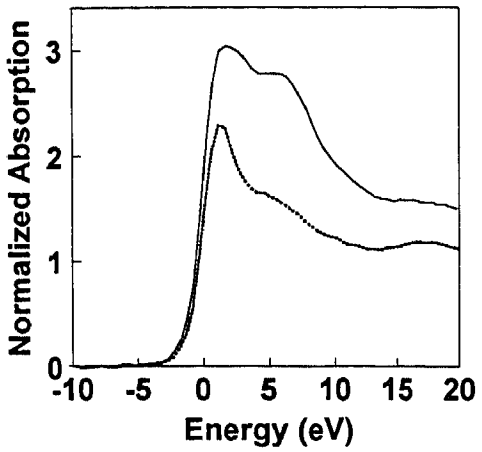

Figure 2. Near Edge Spectra of H-Y (dotted line) and H-USY (solid line).

3.4 EXAFS Data

The EXAFS data for H-USY (solid line) and previously reported NaY (dotted line) [10,11] are given in Figure 3a. The EXAFS data of NaY is characteristic of pure Al_{tet} while H-USY contains about 60% Al_{tet} and 40% Al_{oct}. Figure 3a shows that at k values above 3.5 $Å^{-1}$ the nodes of the EXAFS functions of H-USY are shifted to lower values compared to NaY consistent with the different Al-O coordinations. In addition, the amplitude of the EXAFS function is lower in H-USY. The differences in the EXAFS spectra are seen more clearly in the Fourier transforms, Figure 3b, H-USY (solid line) and NaY (dotted line). The imaginary part of the Fourier transform between 1.5 and 2.0 Å in H-USY is shifted to higher values of r, while the magnitude of the Fourier transform is much lower and broader due to the presence of the Al_{oct}.

Comparison of the EXAFS data and Fourier transforms for H-USY (solid line) and H-Y (dotted line) are shown in Figure 4. The node positions of the EXAFS functions in H-USY are shifted to slightly lower values of k compared to H-Y although the shift is smaller in H-Y than NaY, Figure 4a. Differences in the positions of the magnitude and the imaginary parts of the Fourier transforms of H-USY and H-Y can be seen in Figure 4b.

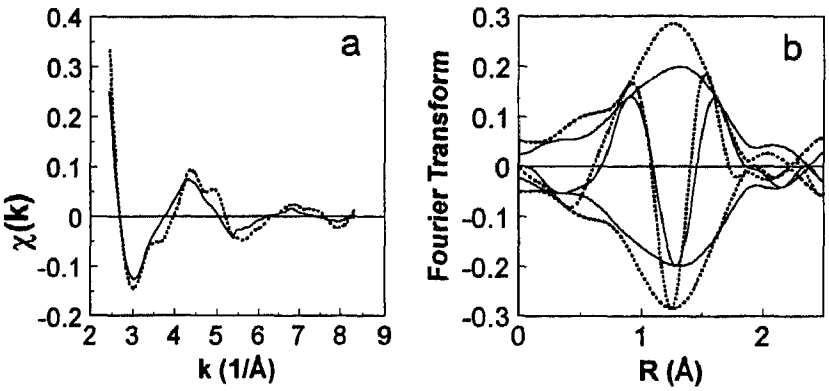

Figure 3. a.) EXAFS spectra of NaY (dotted line) and H-USY (solid line), b.) Fourier transform (k^1, Δk=2.7-8.3 $Å^{-1}$) of data in 3a.

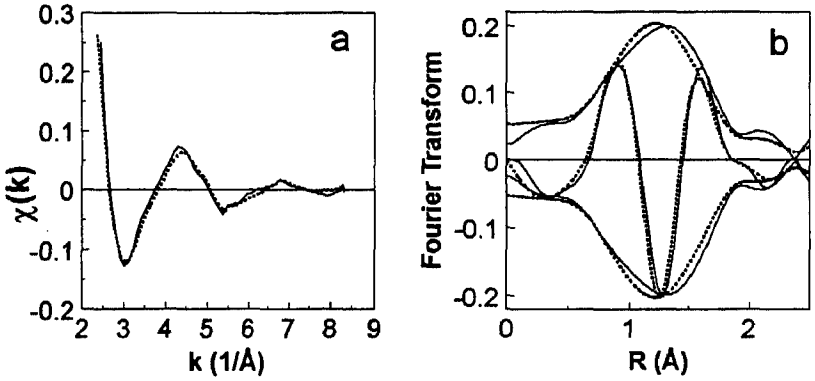

Figure 4. a.) EXAFS spectra of H-Y (dotted line) and H-USY (solid line), b.) Fourier transform (k^1, Δk=2.7-8.3 $Å^{-1}$) of 4a.

3.5 EXAFS Structural Analysis

The EXAFS data of H-Y were previously analyzed using a k-space fit and assuming that the presence of the 15% Al_{oct} did not significantly affect the coordination parameters of the Al_{tet} [10]. An r-space fit allows for the use of a larger data range leading to more reliable analysis [16]. The results of the single shell r-space fit for H-Y are given in the Table. In the fitting procedure, the k weighting and data ranges for all samples were identical (k^1, Δk = 2.7-8.2 $Å^{-1}$, Δr = 0.5-2.5 Å).

Using the fraction of Al_{tet} and Al_{oct} from the ^{27}Al NMR and the true coordination numbers, the EXAFS coordination numbers were calculated and used as fixed input parameters in the model fit. For example, the EXAFS coordination number of Al_{oct} is 0.9 (0.15 x 6). The remaining parameters were optimized by the non-linear, multiple shell fitting procedure (Table). The Al-O distance of 1.71 Å for the Al_{tet} for the single shell fit is slightly

longer than the 1.69 Å for the two shell fit. The higher Debye-Waller factor for Al_{tet} (0.003 vs. -0.002 Å^2) indicates a higher structural disorder and is due inclusion of the Al_{oct} in the single shell fit. The Al_{oct}-O distance is 1.91 Å, and the Debye-Waller factor is -0.009.

Because of the uncertainty of the structure associated with the 30 ppm ^{27}Al NMR resonance in H-USY [16-17], the fraction of Al_{tet} and Al_{oct} can not be determined by NMR. From the XRD, however, the fractions of (structural) Al_{tet} and Al_{oct} are estimated to be 60% and 40%, respectively. Using these fractions, estimated EXAFS coordination parameters were calculated as above. Based on these initial values, the EXAFS coordination numbers were optimized along with the other fitting parameters in the multiple shell fit (Table). Comparison of the multiple shell fit with the isolated first shell EXAFS data are shown in Figure 5. The quality of the other fits was similar. The Al-O coordination distance for Al_{tet} in H-USY (1.67 Å) is slightly shorter than that in H-Y (1.69 Å). In addition, the Debye-Waller factor is much smaller in H-USY (-0.011 Å^2). The Al-O coordination distance for Al_{oct} in H-USY (1.84 Å) is also shorter than that in H-Y (1.91 Å), while the Debye-Waller factor is similar for both zeolites.

Table
Coordination Parameters

Compound	Coordination	N	R (Å)	$\Delta\sigma^2$ (Å^2)	ΔE_o (Å)
H-Y (single shell fit)	Al-O	4.1	1.71	0.003	0.6
H-Y (two shell fit)	Al_{tet}-O	3.2*	1.69	-0.002	-1.2
	Al_{oct}-O	0.9*	1.91	-0.009	-1.9
H-USY	Al_{tet}-O	2.2	1.67	-0.011	-2.5
	Al_{oct}-O	2.3	1.84	-0.012	-2.2

*Fixed input parameters.

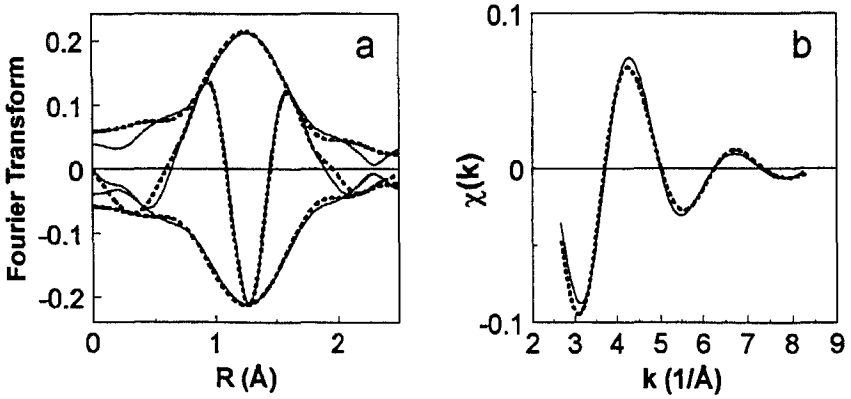

Figure 5. R-space fit (k^1, Δk=2.7-8.2 Å^{-1}, Δr=0.5-2.5 Å) of H-USY a.) Fourier transform of data (solid line) and fit (dotted line), b.) Fourier filtered data of 5a.

4. DISCUSSION

4.1 EXAFS

The Al EXAFS data range is limited up to about k = 8.5 $Å^{-1}$ due to the overlap of the Si K absorption edge. Fitting in k-space reduces the effective data range to about 3.5 Å [10] due to the window effect caused by Fourier filtering of the first coordination shell [16]. Direct fitting in r-space avoids Fourier filtering extending the useful datal range to about 5.5 Å. The larger data range increases the accuracy of the analysis and allows for a two shell fit, i.e., an increase in the number of independent parameters allowed in the fit. In order to reliably resolve the two different Al-O coordinations, the fit must include the imaginary part of the Fourier transform as well as the magnitude of the Fourier transform since the imaginary part is much more sensitive to the coordination distance, see Figures 3b and 4b.

In order to separate the two Al-O contributions in the EXAFS, additional information is required about the relative amounts of Al_{tet} and Al_{oct}. When the fraction of Al_{oct} is about 0.5, the EXAFS coordination numbers can be independently determined from a two shell fit. However, the best fit is obtained if the fractional coordination numbers are estimated from alternative techniques, like NMR and XRD, and optimized during the fitting process. If the fraction of Al_{oct} is low as in H-Y, the contribution to the EXAFS is small. In this case, the EXAFS coordination numbers estimated from NMR (or XRD) are input as fixed parameters into the two shell fit.

Accounting for the small amount of Al_{oct} in H-Y, the Al_{tet} coordination distance decreases slightly from 1.71 Å in the single shell fit compared to 1.69 Å in the multiple shell fit. The Al-O bond distance in H-Y is within the accuracy of the analysis equivalent to that in NaY, H-CaY and H-LaY (1.70 Å) [11], therefore the Al-O distance is independent of the type of cation, or acid strength, at least when the amount of framework Al is identical. In H-USY, the Al_{tet} coordination distance is 1.67 Å, slightly shorter than in H-Y and may be due to the increase in Si/Al ratio. The octahedral Al-O distance in H-Y is 1.91 Å and is similar to that in γ-AlOOH (boehmite) and other aluminum oxides (1.91 Å) [17]. The Al_{oct} distance in H-USY is 1.84 Å which is considerably shorter than in H-Y and suggests that the Al coordination environment is very different in the two zeolites. The calculated Al_{tet} EXAFS functions in H-Y (dotted) and H-USY (solid line) are shown in Figure 6a and show that the node positions in H-USY are different. The calculated Al_{oct} EXAFS functions in H-Y and H-USY are shown in Figure 6b. Again the differences are sufficiently large to be distinguished. It is estimated that coordination distances of 0.01 Å can be resolved. In a previous Al EXAFS study of H-USY, the Al-O bond distance increased to 1.8 Å and coordination number increased to 6 following steam dealumination. In that study, however, all Al were considered to have the same coordination environment [18]. Inclusion of the longer Al_{oct} distance would increase the average Al-O distance in dealuminated Y.

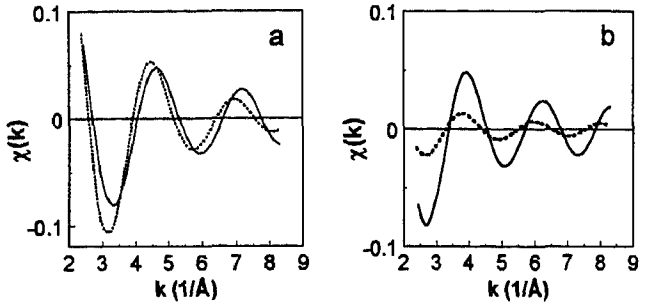

Figure 6. Calculated EXAFS function of Al_{tet} of H-Y (dotted line) and H-USY (solid line), b.) calculated EXAFS function of Al_{oct} of H-Y (dotted line) and H-USY (solid line).

Comparison of the calculated EXAFS functions for Al_{tet} and Al_{oct} are shown in Figure 7a for H-USY. The EXAFS functions of Al_{tet} (solid line) and Al_{oct} (dotted line) are nearly opposite in phase above k = 7 $Å^{-1}$. As a result, the amplitude of the EXAFS which is the sum of the two contributions (dashed line) is enhanced at low k, but is diminished at high k. The corresponding Fourier transforms are shown in Figure 7b. A similar effect occurs for H-Y although the amount of Al_{oct} is much lower. These changes in the amplitude of the EXAFS function lead to a larger Debye-Waller factor in the single shell analysis in H-Y. In addition, the anti-phase character of the two Al contributions results in a lower amplitude in the magnitude of the Fourier transform. In Figure 3b, for example, the amplitude of the Fourier transform of NaY which has only tetrahedral Al is greater than that of H-USY which contains both octahedral and tetrahedral Al.

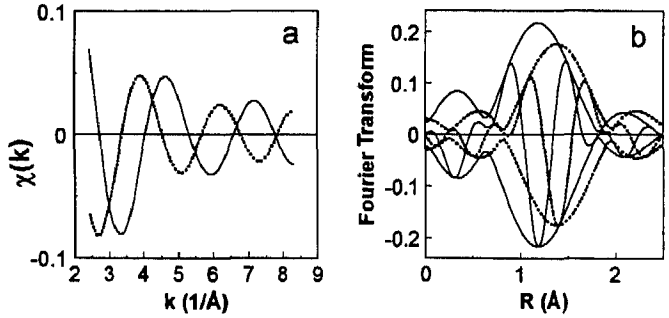

Figure 7. a.) Calculated EXAFS functions of Al_{tet} (solid line) and Al_{oct} (dotted line) in H-USY, b) Fourier transform (k^1, Δk=2.7-8.2 $Å^{-1}$) of the EXAFS data in 7a.

The EXAFS coordination numbers for Al_{tet} and Al_{oct} in H-USY were 2.2 and 2.3, respectively. From the actual coordination numbers, the fractional occupancy from the EXAFS data is calculated to be 0.55 Al_{tet} and 0.38 Al_{oct} which is in good agreement with the XRD determination. The fraction of Al_{oct} also agrees with the ^{27}Al NMR data. The fraction of Al_{tet} from EXAFS, however, is larger than that from Al NMR e.g., 0.4. If the 30 ppm

resonance in the NMR were due to tetrahedral Al, then the total Al_{tet} determined by NMR would be 0.55, in good agreement with both XRD and EXAFS results. We conclude that the 30 ppm resonance in the ^{27}Al NMR spectrum is due to tetrahedral Al. Previously, the 30 ppm resonance was assigned to non-structural, tetrahedral Al (14). A 30 ppm Al NMR resonance has also been observed in LaY where it was shown that there was no extra-lattice Al. The 30 ppm peak was assigned to structural (tetrahedral) Al exchanged with La^{+3} ions [19]. The similarity of the NMR in H-USY and La-Y suggests that not only is the 30 ppm resonance in H-USY due to tetrahedral Al, but that this Al is, addtionally, in the lattice adjacent to a highly charge cation located at the ion exchange site. In H-USY, the exchanged cation is octahedral Al^{+3}.

4.2 Whiteline Intensity and Acidity

The position of the Al_{tet} and Al_{oct} near edge spectrum in H-USY are clearly resolved as previously observed (18). The intensity of the whiteline of the Al_{tet} in H-USY is larger than that in H-Y. Since the fraction of Al_{tet} is smaller in H-USY the actual difference is larger than shown in Figure 2b. An increase in whiteline intensity is due to an increasing positive charge, or a lower electron density on the Al ion. Thus, the structural Al ions in H-USY have a much higher positive charge than those in H-Y. In a previous study, it was shown that the whiteline intensity increases in the order HY < H-CaY < H-LaY, implying that the positive charge on the structural Al ions is highest for H-LaY. Since the acidity also increases in the order HY < H-CaY < H-LaY, it was concluded that the whiteline intensity scales with the acidity [11]. The increase in the whiteline intensity of Al_{tet} with increasing acidity is also observed for H-USY and H-Y and confirms the earlier conclusions that the increased acidity parallels the increase in positive charge on the Al_{tet}.

4.3 Model for Enhanced Acidity in H-USY

Two factors are thought to contribute to the enhanced acidity of steam dealuminated Y, the isolation of the acid sites, i.e., the changing Si/Al ratio [3,4], and the presence of non-framework Al [5-9]. The results of this study support the proposal that the some non-framework Al in H-USY is located at ion exchange sites, and that these Al cations withdraw electron density from acidic hydroxyl groups increasing their strength [5]. From the EXAFS and XRD, the 30 ppm Al in the NMR is conclude to be Al_{tet}, i.e., Al in the zeolite lattice. Furthermore, based on the similarity of the Al NMR of H-USY and LaY, these Al are suggested to be adjacent to Al^{+3} cations located at ion exchange sites. The effect of steaming, therefore, is to produce non-framework, octahedral Al some of which is located at cation exchange sites.

Previously, the effect of ion exchange in H-Y, H-CaY and H-LaY was shown to increase the positive charge on the lattice Al as the charge of the cation increased [11]. The order of the Al electron density parallels the acidity of the catalysts. That is, the positive charge on the Al is highest for the most acidic zeolite. It was proposed that polyvalent cations withdraw Al electron density through the coordinated oxygen ions. In addition, it was suggested that the polyvalent cations withdraw electron density from the lattice oxygen increasing the acid strength of nearby hydroxyl groups. Similarly, in H-USY, it is proposed that Al_{oct} ions at cation sites and coordinated to lattice oxide ions withdraw electron density from the Al_{tet}. The Al^{+3} cations would also be expected to withdraw electron density from the lattice oxygen ions, thus, increasing the acid strength of nearby acid sites as previously suggested [5].

5. CONCLUSION

By determination of the fraction of lattice Al from ^{27}Al NMR or XRD, the individual Al-O distances of both structural and extra framework Al can be determined by low energy Al XAFS spectroscopy. In H-Y, the Al_{tet}-O distance is 1.69 Å, while in H-USY the bond distance is slightly shorter, 1.67 Å. The Al_{oct}-O distance in H-Y is 1.91 Å and decreases to 1.84 Å in H-USY. The large increase in the whiteline intensity of the Al_{tet} in H-USY indicates that the structural Al has a higher positive charge than in H-Y which is consistent with the higher acidity of H-USY. The XAFS results, in combination with the ^{27}Al NMR and XRD, suggest that a fraction of the octahedral, non-framework Al in H-USY are Al^{+3} cations located at ion exchanged sites. The results of this study, support the model that the enhanced acid strength in steam dealuminated Y is due to the formation non-framework Al^{+3} cations at ion exchange sites which withdraw electron density from the lattice oxygen increasing the strength of nearby acid sites.

REFERENCES

1. J. Scherzer, Catalytic Materials: Relationship Between Structure and Reactivity, T.E. White, Jr., R.A. Dalla Betta, E.G. Derouane and R.T.K. Baker (eds.), ACS Sym. Ser. **248**, ACS, Washington, 1984, p. 157.
2. M.L. Poutsma, Zeolite Chemistry and Catalysis, J.A. Rabo (ed.), ACS Mon. **171**, ACS, Washington, 1976, p. 437.
3. E. Dempsey, J. Catal., **39** (1975) 155.
4. R.J. Mikovsky and J.F. Marshall, J. Catal., **44** (1976) 170.
5. F. Lonyi and J.H. Lunsford, J. Catal., **136** (1992) 566.
6. C. Mirodatos and D. Barthomeuf, J. Chem. Soc., Chem. Commun., (1981) 39.
7. R.A. Beyerlein, G.B. McVicker, L.N. Yacullo and J.J. Ziemiak, J. Phy. Chem., **92** (1988) 1967.
8. G. Garrolon, A. Corma and V. Fornes, Zeolites, **9** (1989) 84.
9. J. Abbot, Appl. Catal., **47** (1989) 33.
10. D.C. Koningsberger and J.T. Miller, Catal. Lett., **29** (1994) 77.
11. D.C. Koiningsberger and J.T. Mller, Studies of Sur. Sci. and Catal., **97**, Zeolites: A Refined Tool for Desiging Catalytic Sites; L. Bonneviot and S. Kaliaguine, (eds)., Elsevier, (1995) 125.
12. D.W. Breck and E.M. Flannigan, Molecular Sieves, Soc. Chem. Ind., London, (1968) 47.
13. J.-P.Gilson, G.C. Edwards, A.W. Peters, K. Rajagopalan, R.F. Wormsbecher, T.G. Roberie and M. P. Shatlock, J. Chem. Soc., Chem. Commun., (1987) 91.
14. A. Samoson, E. Lippmaa, G. Engelhardt, U. Lohse and H.-G. Jerschkewitz, Chem. Phy. Lett., **134** (1987) 589.
15. G.J.Ray, B.L. Meyers and C. L. Marshall, Zeolites, 7 (1987) 307.
16. M. Vaarkamp, I.Dring, R.J. Oldman, E.A. Stern and D.C. Koningsberger, Phy. Rev. B., **50** (1994) 7872.
17. R.D. Shannon, K.H. Gardner, R.H. Staley, G. Bergeret, P. Gallezot, and A. Auroux, J. Phys. Chem., **89** (1985) 4778.
18. E. Dooryhee, G.N. Grieves, A.T.Steel, R.P. Townsend, S.W. Carr, J.M. Thomas and C.R. Catlow, Farad. Discuss., Chem. Soc., **89** (1990) 119.
19. H. Klein, H. Fuess and M. Hunger, J. Chem. Soc., Farad. Trans., **91** (1995) 1813.